



Analytical approach to the time evolution of rotation of galaxies

E. Casuso¹; J. E. Beckman^{1,2}

¹Instituto de Astrofísica de Canarias, 38205, La Laguna, Tenerife, Spain

²C.S.I.C., Madrid, Spain

E-mail: eca_ext@iac.es

ABSTRACT

We present here an analytical approach to the theoretical model for the time evolution of angular momentum of galaxies presented previously in Casuso and Beckman(2015), where the Coriolis force acting on a galaxy situated at the surface of a rotating cosmic void could play an important role in addition to tidal torques among proto-galaxies to explain the present angular momentum distribution. We use the Emmy Noether theorem in Lagrangian Mechanics to obtain a theoretical relation between the angular momentum of galaxies and the cosmic time, and compare our results with both numerical models and observations.

Subject headings: (cosmology:) large-scale structure of Universe

1. Introduction

It has gradually come to be accepted that the origin of the angular momentum of galaxies can be explained by some variant of Hoyle (1949) and Sciama (1945) idea that protogalaxies are spun up by the tidal fields of their neighbours. The first detailed calculation of the acquisition of angular momentum in the early stages of protogalactic evolution was made by Peebles(1969), who used linear approximation to find the growth rate of the spin angular

momentum contained within a comoving spherical region of the expanding universe. He found that the angular momentum in such regions grows only to second order in the perturbation expansion and in proportion to $t^{5/3}$ for an Einstein-de Sitter universe. But, as was pointed out by Peebles(1969),the angular momentum of a protogalaxy normally grows at first order in proportion to t for a flat universe and Peebles' s result is a consequence of the spherical symmetry he imposed(White1984). The influence of the evolution of galactic angular momentum on the evolution of galaxies was recognized early as a driver of galaxy morphology(Doroshkevich1970, Hoyle1949). Later Peebles(1969)introduced the so called spin parameter $\lambda = \frac{JE^{1/2}}{GM^{2/5}}$ where J is the dark matter halo angular momentum, E the modulus of the energy, and M the total mass of the galaxy. This parameter was studied both analytically and numerically within the framework of hierarchical galaxy formation (Barnes 1987, Heavens 1988, Warren 1992, Catelan 1996). Some authors (Maller 2002, Vitvitska2002, Hetznecker2006)have pointed out that in addition to tidal torquing, galaxy mergers play a driving role in the evolution of galactic spins (we use in this paper spin and angular momentum as synonymous). In the cold dark matter paradigm, baryonic disk galaxies form at the centers of dark matter halos (Fall 1980, Fall 1983). At low redshift several authors(Fall 1983, Dutton 2012, Romanowsky 2012, Fall 2013, Courteau 2015) have studied the angular momenta of both star forming disks and of passive spheroids. Fall(2013) find $j_d/j_{DM} \sim 0.9$ for late type, star forming discs, and ~ 0.3 for early type, passive spheroids, with Sa and S0 galaxies in between these extremes. This suggests loss or redistribution of angular momentum after the gas has entered the virial radius, with spheroidal galaxies suffering a substantial larger amount of loss than disks. The relative fraction of barionic-to-dark matter mass in the half-light regions of $z \sim 0$ galaxies also depends on type and mass. Massive early type spheroidal systems and massive disks, including the Milky Way, are baryon dominated(Courteau2015). In contrast,the dark matter fraction is significant and becomes even dominant for low-mass spheroids(dwarf ellipticals) and lower mass disks (Martinsson2013). In the outer regions(10-30Kpc) $z=0$ disks are dark matter dominated, as shown by their flat rotation curve(Courteau2015). At high z little is known empirically so far about the baryonic angular momentum distribution(Forster2006). In Casuso and Beckman(2015) we presented a theoretical model in which the origin of angular momentum of galaxies begins after recombination epoch, when matter was organized around bubbles or voids which acquired rotation by gravitational tidal torque interaction. Then, a combination of the effects of the gravitational collapse of gas in protogalaxies and the Coriolis force due to the rotation of the voids could produce and maintain the rotation of galaxies. The aim of the present article is to

throw light on the time evolution of the angular momentum of galaxies. It is organized as follows: in Section 2 we present the observational data and numerical simulations used as constraints on the theoretical model; in Section 3 we develop the theoretical model; in Section 4 we compare the predictions of the model with data; and in Section 5 we present our conclusions.

2. Observational data and numerical predictions to compare

The obtaining of angular momentum data of galaxies at high redshift is actually an observational and also theoretical numerical issue of increasing interest. We use to compare with our theoretical predictions in the present paper the latest published results in both: Burkert(2015) and Zavala(2015). Burkert(2015) give us the observational data of angular momenta of massive star forming galaxies at the peak of the cosmic star formation epoch (z between 0.8 and 2.6), by taking advantage of the recent growth in sample sizes and coverage of the stellar mass-star formation rate plane with $H\alpha$ kinematics integral field unit (IFU) data sets. This progress has started in the last few years, for instance with the SINS/zC-SINF(Mancini2011), MASSIV(Epinat2012) and HiZELS(Swinbank2012) surveys with SINFONI on the VLT, as well as with surveys with OSIRIS on the Keck telescope (Glazebrook2013). They also have used the KMOS^{3D} survey (Wisnioski 2015) with the multiplexed near-infrared IFU spectrometer KMOS on the VLT(Sharples2012), which will deliver IFU data for at least 600 star forming galaxies with z between 0.76 and 3. The combined data of these surveys provide a 450 galaxy sample with a good coverage of massive ($\log(\frac{M_G}{M_\odot}) \geq 10$) star forming galaxies in the $z \sim 0.8-2.6$ redshift range. We also compare our results with the last numerical simulation of Zavala et al. (2015). They explore the co-evolution of the specific angular momentum of dark matter haloes and the cold baryons that comprise the galaxies within. They study over two thousand central galaxies within the reference cosmological hydrodynamical simulation of the Evolution and Assembly of Galaxies and their Environments(EAGLE) project. They employ a methodology within which the evolutionary history of a system is specified by the time-evolving properties of the Lagrangian particles that define it at $z=0$.

3. The theoretical model

We begin by constructing the Lagrangian function of a typical galaxy like the Milky Way in

the assumption of a galaxy rotating around one axis, and using the virial theorem to obtain the gravitational potential energy for simplicity:

$$L = E_C - E_P = \frac{1}{2}I_G\omega_G^2 + \frac{GM_G^2}{2R_G} \quad (1)$$

where E_C is the kinetic energy of a rotating galaxy, E_P its potential energy, I_G its inertia momentum, ω_G its angular velocity, M_G its total mass (baryonic and dark), and R_G the radius of the galaxy or protogalaxy. Due to

$$I_G = \frac{1}{2}M_GR_G^2 \quad (2)$$

and that the angular momentum of galaxy is

$$J = M_GR_G^2\omega_G \quad (3)$$

and also due to the Coriolis force on a galaxy like a rotating object on the surface of a rotating cosmic void (Casuso and Beckman 2015):

$$J = M_G2\Omega\sin\phi R_G v \quad (4)$$

where Ω is the angular velocity of the cosmic void, ϕ the angular distance from the void equator, and v the first time derivative of R_G , we have from the equations (3) and (4)

$$\omega_G \simeq 2\Omega \frac{q'}{q} t \quad (5)$$

where we have taken $q = R_G$ and $q' = v$. Then the Lagrangian function of a typical galaxy rotating around one axis and inside the surface of a rotating cosmic void is now:

$$L = M_G\Omega^2 q^2 t^2 + \frac{GM_G^2}{2q} \quad (6)$$

Now, to be realistic, and due to the dynamical friction between the two voids interacting, the rotation decays exponentially as is derived from the proportionality between the time derivative of Ω and Ω (see equation 7.18 of Binney and Tremaine 1987) we have $\Omega \simeq \Omega_0 \exp(-\lambda t)$, where Ω_0 is the Ω at $t = 0$ and $\lambda = \frac{1}{T_B}$ being $T_B \gg T_U$ the time of breaking for the

rotation of a cosmic void and T_U the age of the Universe. Then we can assume $\Omega \simeq \text{constant}$.

Now, following Emmy Noether theorem, we can make the linear transformation $q \rightarrow q + \epsilon = Q$, which assure the condition $[Q]_{\epsilon=0} = q$. Then

$$\left[\frac{\partial Q}{\partial \epsilon} \right]_{\epsilon=0} = q' \left[\frac{\partial T}{\partial \epsilon} \right]_{\epsilon=0} = q' \psi \quad (7)$$

So

$$\left[\frac{\partial T}{\partial \epsilon} \right]_{\epsilon=0} = \frac{1}{q'} \quad (8)$$

and

$$\psi = \frac{1}{q'} \quad (9)$$

$$T = t + \frac{\epsilon}{q'} \quad (10)$$

assuring the Emmy Noether theorem condition that $T|_{\epsilon=0} = t$. Then we have by Emmy Noether theorem that

$$\frac{\partial}{\partial \epsilon} \left[\left(M_G \Omega^2 Q'^2 T^2 + \frac{GM_G^2}{2Q} \right) T' \right]_{\epsilon=0} = F'(t, q, q') \quad (11)$$

where

$$Q' = \frac{dQ}{dT} = \frac{dQ/dt}{dT/dt} = \frac{q'}{T'} = \frac{q'}{1 - \epsilon q''/q'^2} = \frac{q'^3}{q'^2 - \epsilon q''} \quad (12)$$

Then we have

$$\frac{\partial}{\partial \epsilon} \left[M_G \Omega^2 \frac{q'^2}{T'} + \frac{GM_G^2}{2(q + \epsilon)} T' \right]_{\epsilon=0} = F'(t, q, q') \quad (13)$$

So

$$\frac{\partial}{\partial \epsilon} \left[M_G \Omega^2 \frac{q'^4}{q'^2 - \epsilon q''} + \frac{GM_G^2 (q'^2 - \epsilon q'')}{2(q + \epsilon) q'^2} \right]_{\epsilon=0} = F'(t, q, q') \quad (14)$$

And by Emmy Noether theorem

$$\frac{d}{dt} (L\psi) = F' \quad (15)$$

Operating and simplifying equation (14) we have,

$$M_G \Omega^2 q'' - GM_G^2 \left[\frac{q''}{2qq'^2} - \frac{1}{2q^2} \right] = F' \quad (16)$$

And equating (15) and (16) through (6) and (9), we have,

$$\Omega^2 qq''(t^2 - 1) + 2\Omega^2 qq't - \frac{GM_G}{q} = 0 \quad (17)$$

which using $j = 2qq' \Omega t$ taken from equation (5) leads to an expression for the specific angular momentum of a galaxy on the surface of a cosmic void rotating:

$$j = \frac{GM_G}{\Omega q} - \Omega q q''(t^2 - 1) \quad (18)$$

At the other hand, and by comparison, we use the usual expression for the especific angular momentum of a galaxy without Coriolis force:

$$j = q^2 \omega_G \quad (19)$$

with

$$\omega_G \simeq \omega_0 \exp(-t/T_N) \quad (20)$$

being T_N the time scale of decaying galactic angular velocity.

4. Probability distribution of spins of galactic dark matter halos

In order to make a cleaner test our model we must compare our predictions for the probability distribution of spins $P(j)$ of dark matter halos associated to galaxies, with those of cosmological simulations. To do so we follow Casuso and Beckman (2015) and then we derive, in a simple way but with clear physical meaning, a probability distribution of specific angular momentum of dark halos as the product of three effects: one is the consequence of the pure Coriolis effect, and so proportional to $\sin\theta$ where θ is the angle between the equator of void ($\theta=0$) and the rotation axis of the void ($\theta=\pi/2$); the second is the factor $\cos\theta$ due to the assumption that the galaxies formed near the equator of the void have $2\pi R \cos 0$ of length in which to interact directly with galaxies at the surface of the other void in contact and after rotation, while galaxies formed at other latitudes have values $2\pi R \cos\theta$ of length; and the third is the factor associated with a Gaussian function due to the random nature assumed for the relative position of interaction between two voids (equator of one void with equator of the other one, or with the rotation axis, or interaction at any intermediate position angle θ). Then our model predicts:

$$P(j) \propto \sin\theta \cos\theta \exp\left(-\frac{1}{2}\left(\frac{\theta - \theta_0}{\sigma}\right)^2\right) \quad (21)$$

5. Comparison of the model predictions with observations

In Fig. 1 we can see the time evolution of the especific angular momentum of a typical galaxy like the Milky Way, taken from equation (18) with Coriolis Force due to the rotation of the cosmic void hosing the galaxy in its surface. We can compare upper curve (full line)

corresponds to $\Omega = \text{constant}$, and the lower curve (dotted line) is $\Omega \propto \left(\frac{1+z}{4}\right)^{-1/2}$ as in the standard cosmology, with $\frac{1}{1+z} = \left(\frac{3}{2}10^{-10}t\right)^{2/3}$, t in years. We can see how both curves maintain nearly constant the galactic spin. Long dashed line corresponds to equation (19) without Coriolis force and time scale of decaying 10^9 yr. The short dashed line is the result without Coriolis force and time scale of decaying galactic angular velocity 10^8 yr. In Fig. 2 we can see, at lower time scales, the effect of bump (increasing and then decreasing) for the model without Coriolis force, effect which is again obtained by Zavala (2015) for their numerical models (see Fig. 3). Zavala et al.(2015) uses the EAGLE simulation (see Schaye et al. (2015)) which present a full hydrodynamical simulation and a full cosmological setting, but does not include Coriolis effect associated with the rotation of cosmic voids. In fact the EAGLE simulation focuses mainly on the feedback from supernova explosions which would, in principle, play an important role in angular momentum conservation. But as Schaye et al. (2015) point out the importance of physical impact of feedback on angular momentum conservation is not well established. In Fig. 3 we compare our model predictions from eq. (18) with both last numerical model of Zavala et al.(2015) and the observational data. Full line represents the theoretical predictions of the analytical model presented in this paper. Short dashed lines are the limits for the theoretical predictions of Zavala et al. (2015) hydrodynamical numerical EAGLE simulation for disc-dominated galaxies. Long dashed lines are the limits for the theoretical predictions of Zavala et al. (2015) hydrodynamical numerical EAGLE simulation for bulge-dominated galaxies. Full triangles are the limits of Burkert (2015) observational data for star forming galaxies at the peak of the cosmic star formation epoch. Empty squares are the limits for the Romanowsky (2012) observational data for spiral galaxies, including The Galaxy in the range. And empty triangles are the limits for the Romanowsky (2012) observational data for early-type galaxies. We can see how our model explain better the spiral galaxies angular momentum evolution, because the numerical model predictions fall down at present epoch to almost go out of the observational range for spiral galaxies of Romanowsky (2012). And taking into account the broad range of masses of galaxies (from $10^8 M_{\odot}$ to $10^{12} M_{\odot}$) our model (equation 18) predicts a range of 1.3 dex above and below the central value, which include all the data shown in Fig. 3 with the only exception of the smallest values of the range of data from Romanowsky (2012) for early-type galaxies.

6. Conclusions

The most usual results from numerical models are those of the dark matter component of galaxies have angular momenta evolving with time (or with redshift, or with cosmological expansion rate) increasing until some z value and thereafter nearly constant (until now), but for the baryonic component (that observed) predict increasing until some z value like dark matter and thereafter decrease until now. In our model, however, the baryonic component also remains nearly constant (see Fig. 3) until now, due to the supply of angular momentum from cosmic voids to individual galaxies through the Coriolis effect. In a preliminary work Wesson (1981) shown how every object in the universe (planets, doble stars, star clusters, spiral galaxies and superclusters) follow very nearly the same law for the especific angular momentum vs. mass. We can interpret this observational result like a cosmic (global) non-scale hierarchical supply of angular momentum from the big scales (voids) to the lower scales (planets). And the mechanism more simple to do this is the inertial Coriolis force. Although one needs clearly more fine observational data to distinguiss between our model (almost constant angular momentum evolution for spiral galaxies) and the predictions of numerical models, we consider in the present paper a very interesting analytical approach to simplify the comprehension of physics underlying the origin and evolution of angular momentum of galaxies in the Universe.

Figure Captions

Fig. 1.— Time evolution of the especific angular momentum of a typical galaxy such as the Milky Way taken from equation (18) with Coriolis force due to the rotation of the cosmic void which hosts the galaxy on its surface. The units for j are arbitrary. Full line corresponds to $\Omega = \text{constant}$, and dotted line is $\Omega \propto \left(\frac{1+z}{4}\right)^{-1/2}$ as in the standard cosmology, with $\frac{1}{1+z} = \left(\frac{2}{3}10^{-10}t\right)^{2/3}$, t in years. Long dashed line corresponds to equation (19) without Coriolis force and time scale of decaying: 10^9 yr. The short dashed line is the result without Coriolis force and time scale oof decaying for galactic angular velocity: 10^8 yr.

Fig. 2.— The same as in Fig. 1 but in a shorter time scale.

Fig. 3.— Angular momentum of galaxies vs. cosmic time. The especific angular momentum j is shown on a log scale and normalized to the mean value of the observational data for disc-dominated galaxies. Full line represents the theoretical predictions of the analytical model presented in this paper. Short dashed lines are the limits for the theoretical predictions of

Zavala et al. (2015) hydrodynamical numerical EAGLE simulation for disc-dominated galaxies. Long dashed lines are the limits for the theoretical predictions of Zavala et al. (2015) hydrodynamical numerical EAGLE simulation for bulge-dominated galaxies. Full triangles are the limits of Burkert (2015) observational data for star forming galaxies at the peak of the cosmic star formation epoch. Empty squares are the limits for the Romanowsky (2012) observational data for spiral galaxies, including The Galaxy in the range. And empty triangles are the limits for the Romanowsky (2012) observational data for early-type galaxies.

Fig. 4.— Distribution of logarithmic specific angular momentum of dark halos, $j_P(j)$. The solid curve shows our analytic result given by equation (21). The triangles show the Monte Carlo simulations for both non-spherical collapse model and for the Press-Schechter model taken from Chiueh et al. (2002).

Fig. 1.

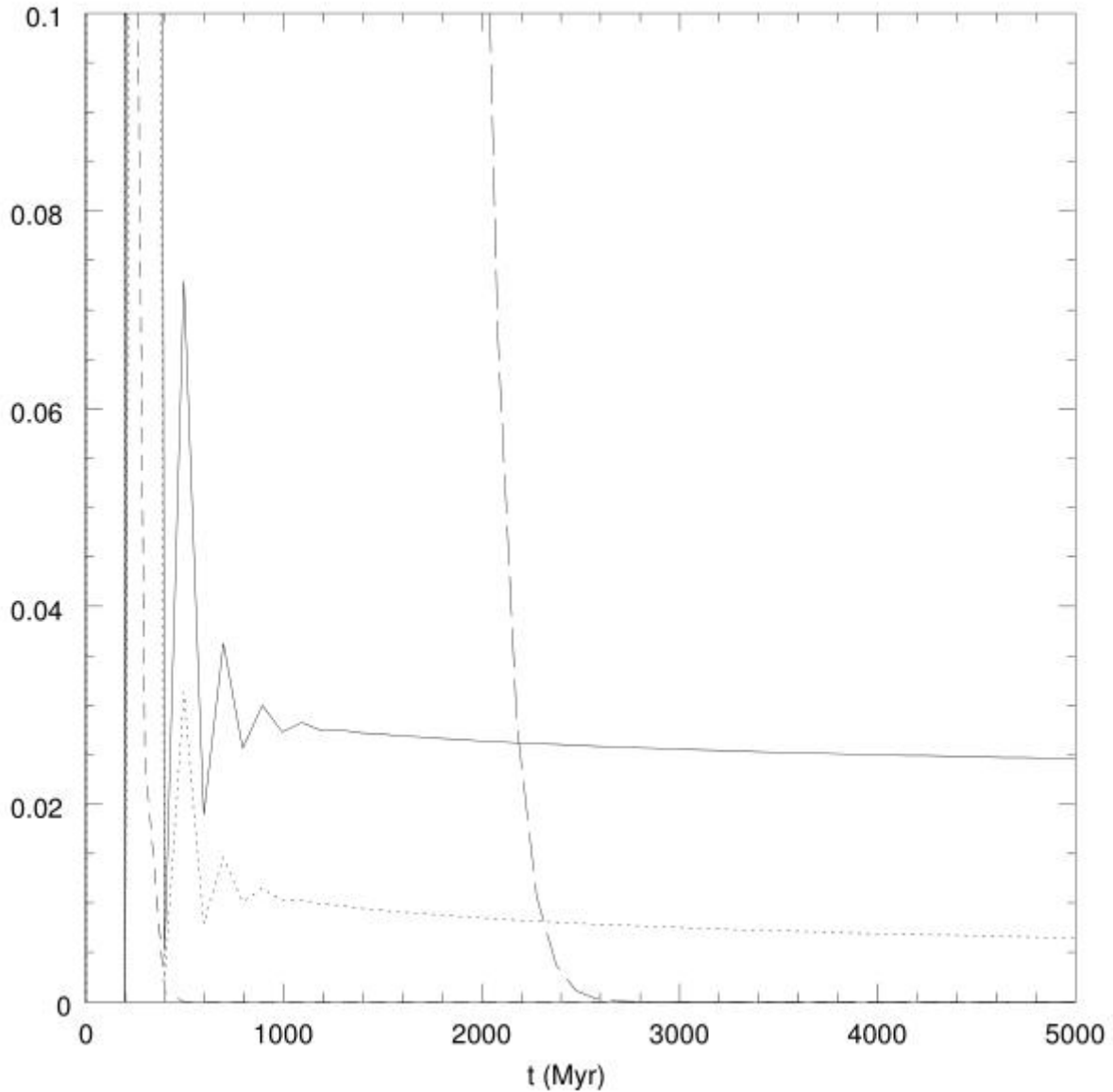


Fig. 2.

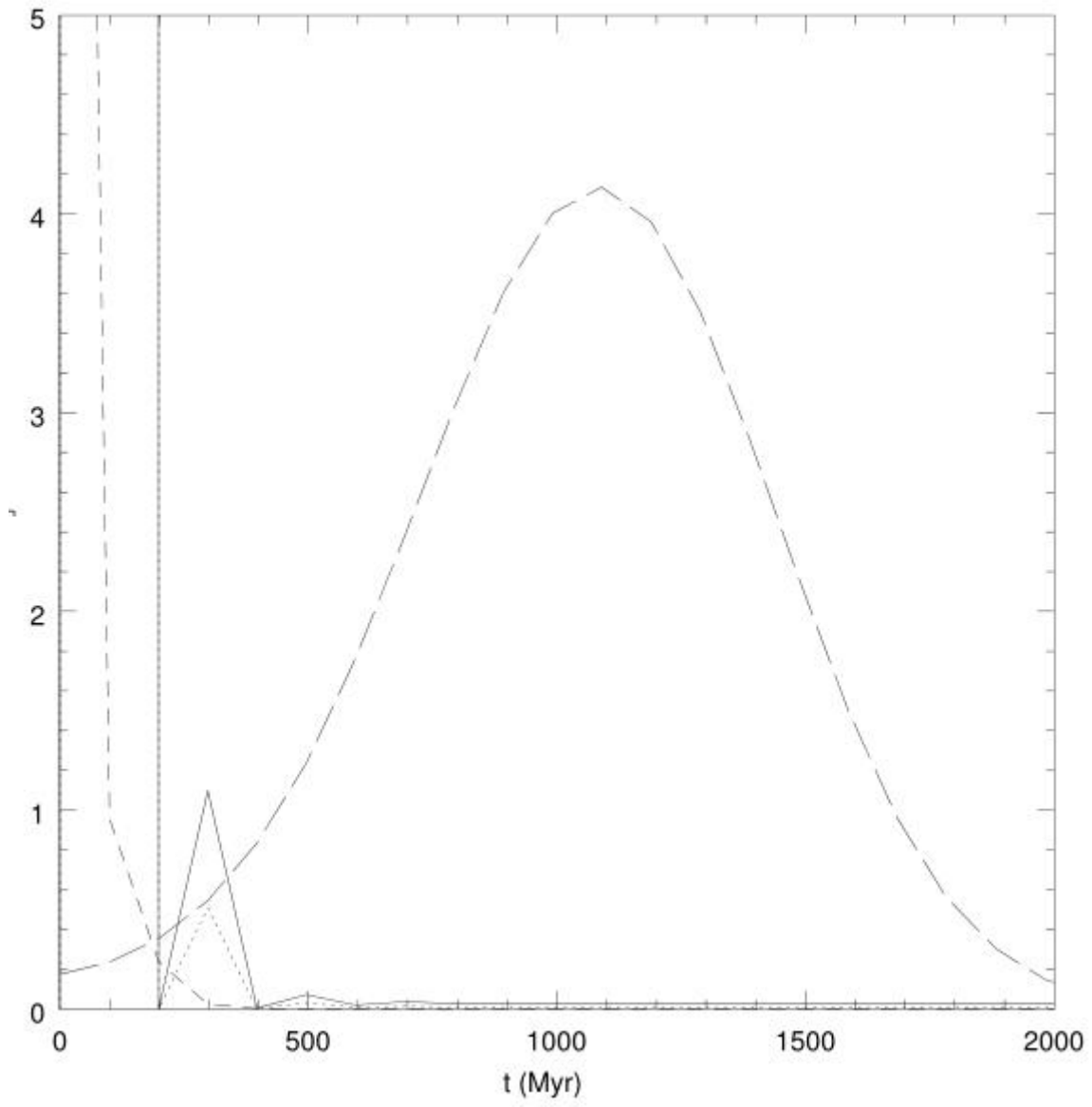


Fig. 3.

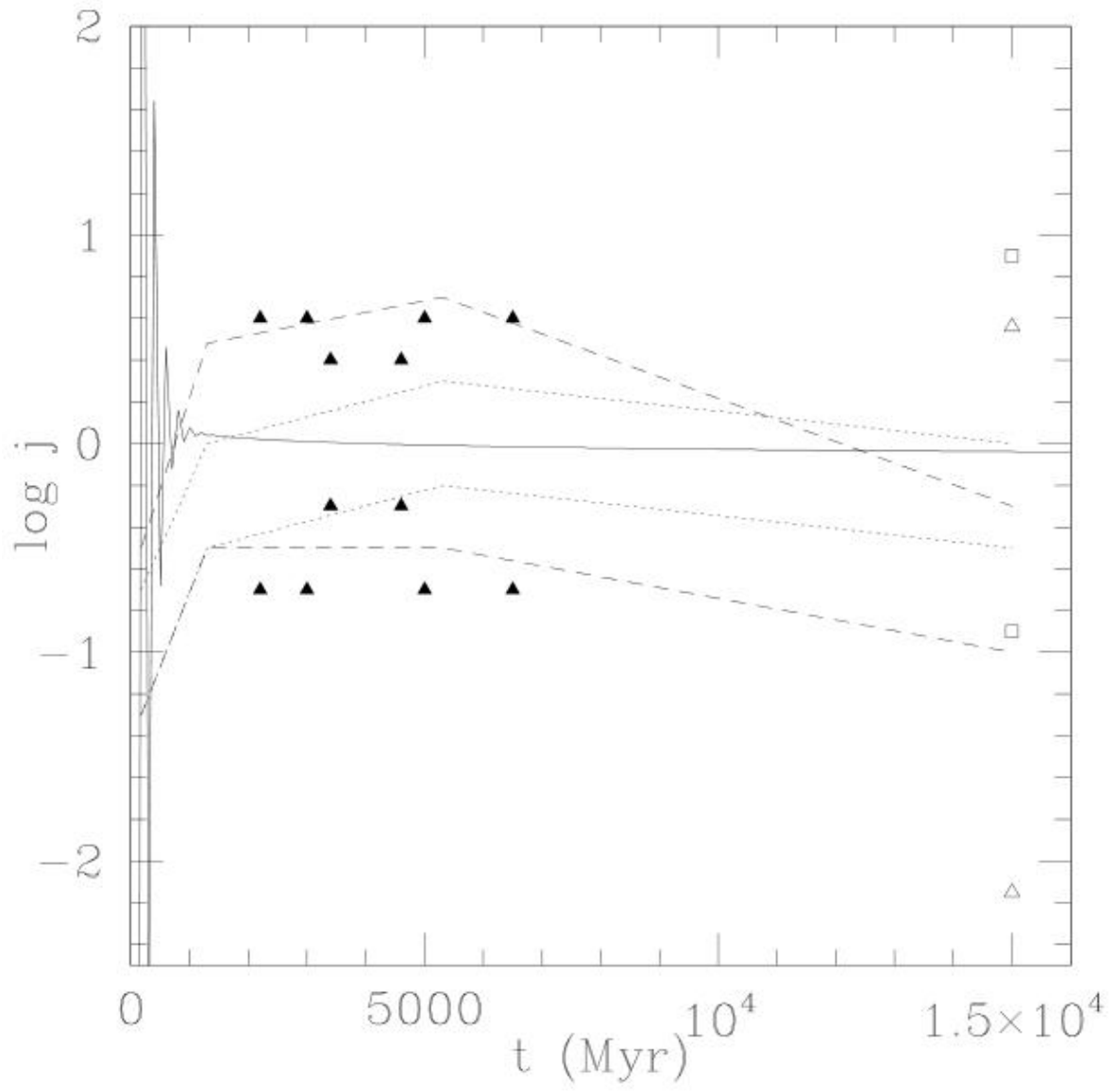
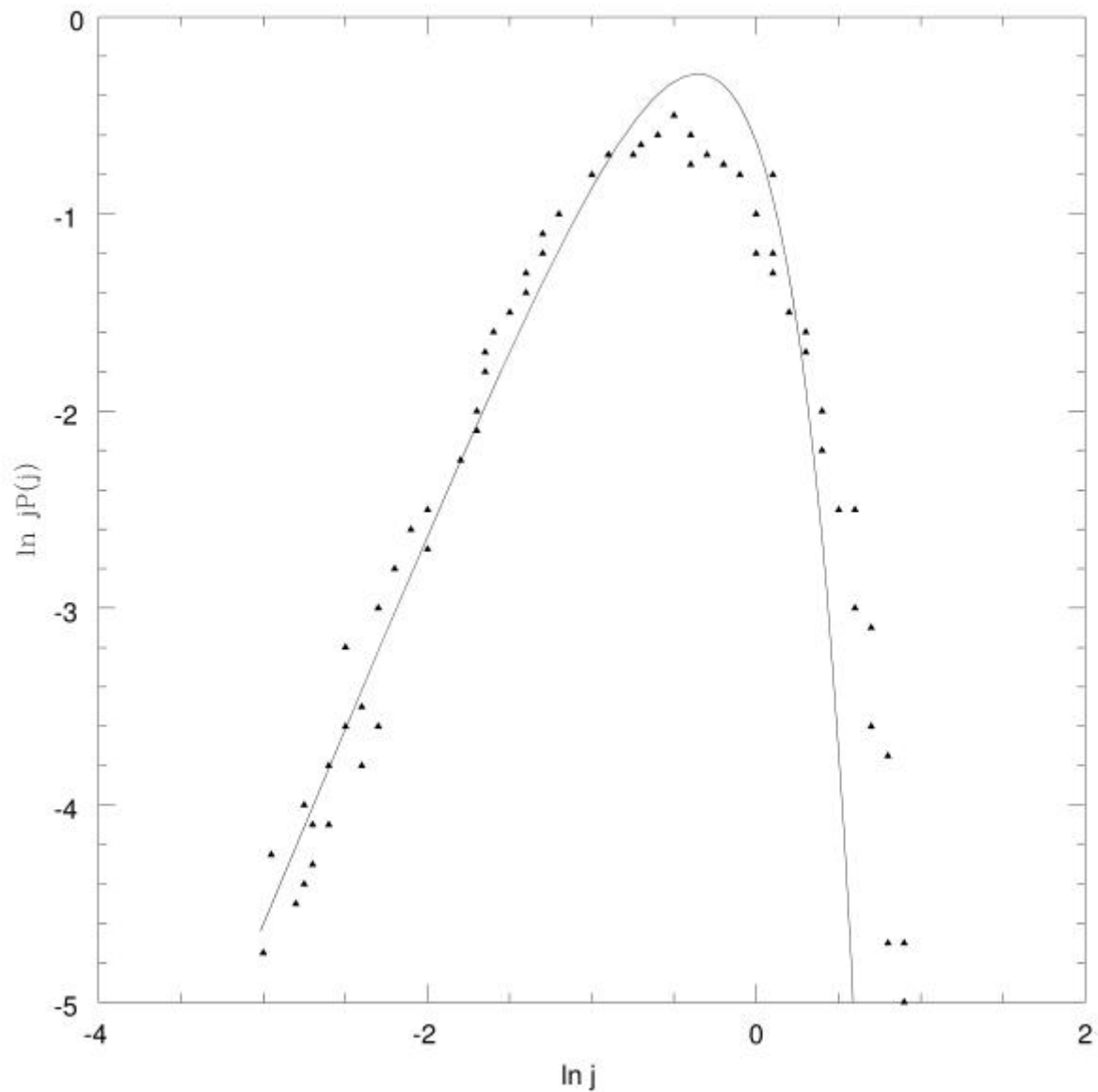


Fig. 4.



REFERENCES

- [1] Barnes, J., Efstathiou, G. 1987, *ApJ*, 319, 575
- [2] Binney, J., Tremaine, S. 1987, "Galactic Dynamics", Princeton Univ. Press
- [3] Burkert, A., et al. 2015, arXiv151003262B
- [4] Casuso, E., Beckman, J. E. 2015, *MNRAS*, 449, 2910
- [5] Catelan, P. Theuns, T. 1996, *MNRAS*, 282, 436
- [6] Chiueh, T., Lee, J., Lin, L. 2002, *ApJ*, 581, 794
- [7] Courteau, S., Dutton, A. A. 2015, *ApJ*, 801, L20
- [8] Doroshkevich, A. G. 1970, *Astrofisika*, 6, 581
- [9] Dutton, A. A., van den Bosch, F. C. 2012, *MNRAS*, 421, 608

- [10] Epinat, B., et al. 2012, *A&A*, 539, 92
- [11] Fall, S. M., Efstathiou, G. 1980, *MNRAS*, 193, 189
- [12] Fall, S. M. 1983, *IAUS*, 100, 391
- [13] Fall, S. M., Romanowsky, A. J. 2013, *ApJ*, 769, L26
- [14] Forster Schreiber, N. M., et al. 2006, *ApJ*, 645, 1062
- [15] Glazebrook, K. 2013, *PASA*, 30, 56
- [16] Godel, K. 1949, *Rev. Mod. Phy.* Vol. 21, 447
- [17] Heavens, A., Peacock, J. 1988, *MNRAS*, 232, 339
- [18] Hetzner, H., Burkert, A. 2006, *MNRAS*, 370, 1905
- [19] Hoyle, F. 1949, in *Problems of Cosmical Aerodynamics* eds. J. Buergers and H. van de Hulst (Dayton, Ohio: Central Air Documents Office), p. 195
- [20] Maller, A. H., Dekel, A., Somerville, R. 2002, *MNRAS*, 329, 423
- [21] Mancini, C., et al. 2011, *ApJ*, 743, 86
- [22] Martinsson, T. P. K., et al. 2013, *A&A*, 557, 131
- [23] Peebles, P. J. E. 1969, *ApJ*, 155, 393
- [24] Romanowsky, A. J., Fall, S. M. 2012, *ApJS*, 203, 1750
- [25] Schaye, J. 2015, *MNRAS*, 446, 521
- [26] Sciamma, D. W. 1955, *MNRAS*, 115, 2
- [27] Sharples, R., et al. 2012, in *Ground-based and Airborne Instrumentation for Astronomy IV*, proceedings of the SPI 8446, 9
- [28] Swinbank, A. M., et al. 2012, *MNRAS*, 426, 935
- [29] Vitvitska, M., Klypin, A. A., Kravtsov, A. V., Wechsler, R. H., Primack, J. R., Bullock, J. S. 2002, *ApJ*, 581, 799
- [30] Warren, M. S., Quinn, P. J., Salmon, J. K., Zurek, W. H. 1992, *ApJ*, 399, 405
- [31] Wesson, P. S. 1981, *Phys. Rev. D*, Vol. 23, 8, 1730
- [32] White, S. D. M. 1984, *ApJ*, 286, 38
- [33] Wisnioski, E., et al. 2015, *ApJ*, 799, 209
- [34] Zavala, J. et al. 2015, *arXiv151202636Z*